Anomalous Hall effect in amorphous $Co_{40}Fe_{40}B_{20}$

Gang Su,[1,2] Yufan Li,[1] Dazhi Hou,[1] Xiaofeng Jin,[1,*] Houfang Liu,[3] and Shouguo Wang[3]

[1]*State Key Laboratory of Surface Physics and Department of Physics, Fudan University, Shanghai 200433, China and Collaborative Innovation Center of Advanced Microstructures, Nanjing University, Nanjing 210093, China*

[2]*College of Mathematics, Physics and Information Science, Zhejiang Ocean University, Zhoushan 316000, China*

[3]*State Key Laboratory of Magnetism, Beijing National Laboratory for Condensed Matter Physics, Institute of Physics, Chinese Academy of Sciences, Beijing 100190, China*

(Received 26 July 2014; revised manuscript received 20 November 2014; published 3 December 2014)

The anomalous Hall effect (AHE) in the "dirty region" ($\sigma_{xx} < 10^4$ S/cm) is studied in amorphous $Co_{40}Fe_{40}B_{20}$ (CoFeB) thin films. Ostensively the conventionally adopted scaling ($\sigma_{AH} \propto \sigma_{xx}^{1.6}$) appears to be valid, but we find that the results can be better explained by the proper scaling [$\sigma_{AH} = -(\alpha\sigma_{xx0}^{-1} + \beta\sigma_{xx0}^{-2})\sigma_{xx}^2 - b$]. This implies that the AHE in the dirty region can also be well described by the standard skew scattering, side jump, and the intrinsic mechanisms.

DOI: 10.1103/PhysRevB.90.214410 PACS number(s): 72.15.Cz, 73.50.Jt, 73.90.+f, 75.47.Np

The anomalous Hall effect (AHE), which is a conventional transport measurement widely used to verify the behavior of magnetization in magnetic semiconductors [1–3] and field effect transistor devices [4,5], has attracted lots of attention in recent years along with the development of spintronics. Particularly, it is believed to share the same mechanism with the spin Hall effect, which can realize a conversion between charge and spin currents, and plays the key role in the next-generation spintronics. Moreover, the physics underlying this spin-dependent transport phenomena is complex and intriguing.

It is known that the AHE has versatile origins resulting from either the extrinsic impurity scattering processes [6,7], or spin-orbit coupling together with interband mixing [8], also known as the Berry curvature contribution or the intrinsic mechanism [9]. Different mechanisms emerge as being dominant in the specific regimes defined by the longitudinal conductivity σ_{xx} [10–12]: for the high conductivity or "clean" regime of $\sigma_{xx} > 10^6$ S/cm, the extrinsic mechanism of skew scattering dominates; for the intermediate metallic regime of 10^4 S/cm $< \sigma_{xx} < 10^6$ S/cm, the intrinsic mechanism dominates. In these two regimes, the different dominating mechanisms of the AHE manifest the anomalous Hall conductivity (AHC) as $\sigma_{AH} \sim \sigma_{xx}^{\xi}$, while $\xi = 1$ or 0, respectively. However, in the lower end or the so-called "dirty regime," where $\sigma_{xx} < 10^4$ S/cm, experiments exhibit an unexpected scaling relation of $\xi = 1.6$ in various ferromagnetic "bad" metals and semiconductors such as Fe_3O_4 [13,14], $Nd_2(Mo_{1-x}Nb_x)_2O_7$, $La_{1-x}Sr_xCoO_3$ [11,15], etc. Although the nonintegral exponent could be reproduced by numerical calculations [10], it provides little understanding on the underlying mechanism [16]. Attempts have been made in searching for the microscopic mechanism by involving the phonon-assisted hopping mechanism and percolation theory [17]. The origin of the AHE in the dirty regime has remained confusing and a major challenge in fully understandingy the phase diagram of the AHE.

Recent studies shed new light on the basic mechanisms of the AHE and showed that different scattering processes contribute to the AHE very differently [18–20]. The extrinsic AHE is found to be dominated by contributions made from elastic scattering processes between the carriers and the impurities, while the inelastic scattering induced by the phonon hardly contributes. Therefore in order to obtain the correct scaling of the AHE that reflects the underlying mechanisms, different scattering processes and their corresponding contribution to the extrinsic AHE should be discriminated. In other words, the value of ξ should only be discussed in the context of knowing what kinds of scattering are included in the experimentally measured σ_{xx}, for instance, whether it is the residual conductivity σ_{xx0} at the lowest accessible temperature that only involves the impurity scattering, or is it the conductivity at a finite temperature that also involves the phonon induced scattering processes (temperature-dependent scattering). With this new understanding, the AHE in a number of ferromagnetic metals and metallic alloys were studied, in which the different mechanisms were clearly distinguished [19,21–24]. We shall now take this advance into the dirty regimewith the hope to unearth the underlying mechanisms of the AHE hidden in the empirical $\xi = 1.6$ scaling law.

The CoFeB alloy is a widely used ferromagnetic material in spintronics, which has been intensively studied for its use in magnetic tunnel junctions [25–28]. So far in these studies the CoFeB layer serves as the ferromagnetic electrode; however, recent progress shows that ferromagnetic material can also be used as a spin current detector by the inverse spin Hall effect [29]. Compared with the extensively studied magnetic properties, little effort is made to investigate such spin-related electron scattering process in CoFeB, which is of possible application in future spin-based devices [30,31]. With carefully designed experiments tuning the impurity scattering and the temperature-dependent scattering (like phonon) independently, we found that under the apparent $\sigma_{AH} \propto \sigma_{xx}^{1.6}$ scaling, the AHE in the amorphous CoFeB thin films can be well explained by the combination of the extrinsic and the intrinsic mechanisms.

The amorphous $Co_{40}Fe_{40}B_{20}$ thin films of various thicknesses are grown by rf sputtering on oxidized Si(001) substrate at room temperature. A 10-nm-thick SiO_2 capping layer is then deposited to prevent oxidation in air. After being transferred out of the growth chamber, each film is patterned

*Corresponding author: xfjin@fudan.edu.cn

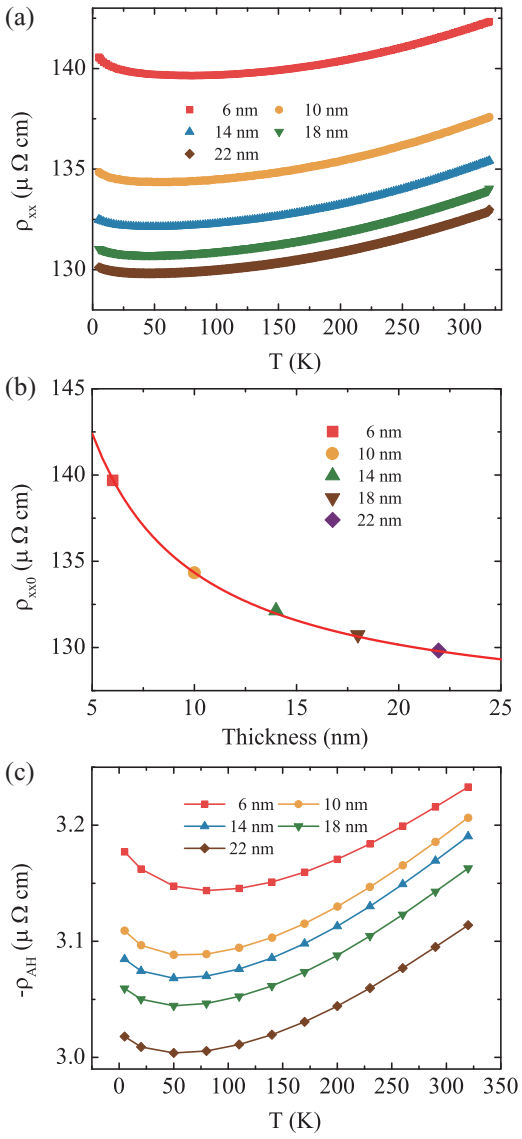

FIG. 1. (Color online) (a) The temperature dependence of the longitudinal resistivity for various CoFeB film thicknesses. (b) The residual resistivity ρ_{xx0} (taken at 50 K) as a function of thickness. The red line is a fitting curve using the Cottey model [32]. (c) The anomalous Hall resistivity versus temperature for various film thicknesses.

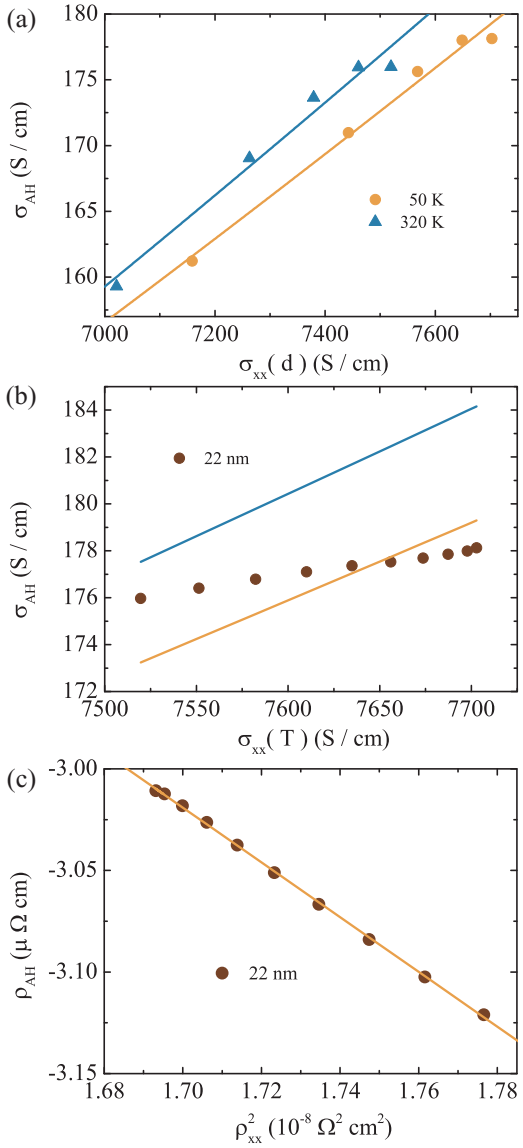

FIG. 2. (Color online) (a) The plot of σ_{AH} versus σ_{xx} (varying with thickness: d) for 50 K (blue dots) and 320 K (yellow dots), with the fitting following ($\sigma_{AH} = A\sigma_{xx}^{1.6} + C$). (b) The plot of σ_{AH} versus σ_{xx} (varying with temperature: T), with the linear fitting with same parameter A and C for 50 K (blue line) and 320 K (yellow line). (c) ρ_{AH} vs ρ_{xx}^2 plot for 22 nm thickness for various temperatures.

into a standard Hall bar. The transport measurements of the longitudinal resistivity ρ_{xx} and the Hall resistivity ρ_{xy} are conducted utilizing a physical property measurement system.

Figure 1(a) shows the temperature dependence of ρ_{xx} for different thicknesses. It is clear that there happens some kind of localization below 50 K. In the following we shall take the ρ_{xx} measured at 50 K as the residual resistivity ρ_{xx0}, as it most truthfully reflects the impurity scattering. In Fig. 1(b) it is seen that this residual resistivity can be tuned by varying the film thickness, due to the finite size effect of the interface scattering [22,32]. Meanwhile for each film with fixed thickness, the temperature-dependent resistivity controls the electron-phonon scattering. Therefore, the current approach provides a clear-cut method to independently control the impurity scattering. Figure 1(c) shows ρ_{AH} as a function of temperature for films at different thicknesses, which is derived from the intercept when extrapolating the ρ_{xy} versus H curves from the high magnetic field to the zero field. From these data we can find the anomalous Hall angle ($\theta_{AHE} = \rho_{AH}/\rho_{xx}$) of CoFeB is about -0.023 in the temperature and thickness range we studied.

As a demonstration of the empirical $\xi = 1.6$ scaling for the materials whose conductivity falls in the dirty regime, we first show the AHC (σ_{AH}) of all the film thicknesses as a function of σ_{xx}, obtained at lowest and highest temperatures in this experiment, i.e., 50 and 320 K, respectively, as plotted in Fig. 2(a). Indeed, the data fits quite well with the curve $\sigma_{AH} \propto \sigma_{xx}^{1.6}$ ($\sigma_{AH} = A_{50,320\,K}\sigma_{xx}^{1.6} + C_{50,320\,K}$). However, for a given

film with fixed thickness, here we take a 22 nm sample as a representative case, the experimentally measured data between σ_{AH} and σ_{xx} [as a function of temperature using the same parameter ($A_{50,320\,K}$ and $C_{50,320\,K}$)] show clear deviation from the $\sigma_{AH} \propto \sigma_{xx}^{1.6}$ scaling as seen in Fig. 2(b), suggesting that the $\xi = 1.6$ scaling does not apply to the temperature dependence of the AHE in CoFeB. Meanwhile, note that σ_{xx}, or ρ_{xx} to be more straightforward, involves both the impurity scattering at low temperature and the electron-phonon scattering at higher temperature. The plot such as Fig. 2(a) seems to imply that these two scattering mechanisms contribute equally to the AHE, which is not impossible but highly unlikely according to our previous discussion [19]. To be more specific, the proper scaling proposed to describe the AHE in the clean and moderate dirty regimes is [19,21–24,33]

$$\rho_{AH} = \left(\alpha\rho_{xx0} + \beta\rho_{xx0}^2\right) + b\rho_{xx}^2, \tag{1}$$

where α and β denote the parameters for the two extrinsic AHE mechanisms, the skew scattering [6] and the side jump [7], respectively; and b denotes the intrinsic AHC. Equation (1) shows that the extrinsic anomalous Hall resistivity is only related to ρ_{xx0}, or the impurity scattering [34]; while the electron-phonon scattering only goes into the intrinsic anomalous Hall resistivity. A better idea is to investigate the dependence of the AHE on only one of the two scattering processes, while the other one is fixed. When the temperature is changed for a film with specific thickness, the residual resistivity is fixed but the electron-phonon scattering is varied. In this case, the first two terms on the right side of Eq. (1) are fixed to be constant, while the third term varies with the temperature. Therefore Eq. (1) reduces to $\rho_{AH} = \text{const} + b\rho_{xx}^2$. To find out if this fits to our CoFeB films, in Fig. 2(c) we plot ρ_{AH} versus ρ_{xx}^2 for the same 22-nm-thick film. The excellent agreement between the experimental data and the linear fitting curve suggests that the intrinsic AHE is present as one of the origins of the AHE in CoFeB. The intrinsic AHC b and the constant term $\alpha\rho_{xx0} + \beta\rho_{xx0}^2$ can be derived from the fitting parameters, the slope and the intercept, respectively.

From another perspective, we can tune the impurity scattering while minimally affecting the electron-phonon scattering. This is achieved, as discussed previously, by tuning the residual resistivity via the film thickness. At 50 K, ρ_{xx} is by definition just the ρ_{xx0}, and therefore Eq. (1) can be converted to $\rho_{AH0}/\rho_{xx0} = \alpha + (\beta + b)\rho_{xx0}$. The subscript "0" denotes the lowest temperature 50 K. In Fig. 3(a) we plot ρ_{AH0}/ρ_{xx0} as a function of ρ_{xx0} for various film thicknesses; these data can be fitted by a straight line as shown by the red line in the figure, from which one can deduce α as the intercept, and $\beta + b$ as the slope. Combining the value of b derived previously, we shall be able to derive β. So far all three unknown parameters involved in Eq. (1) have been obtained.

Now we shall be able to reach the conclusion that the AHE in CoFeB films can be described by Eq. (1). To be more straightforward, we shall present the experimental result in the context of conductivity, which provides a direct comparison to the $\sigma_{AH} \propto \sigma_{xx}^{1.6}$ scaling and helps to clarify the essence of the AHE that is missed in the empirical scaling law. In the form

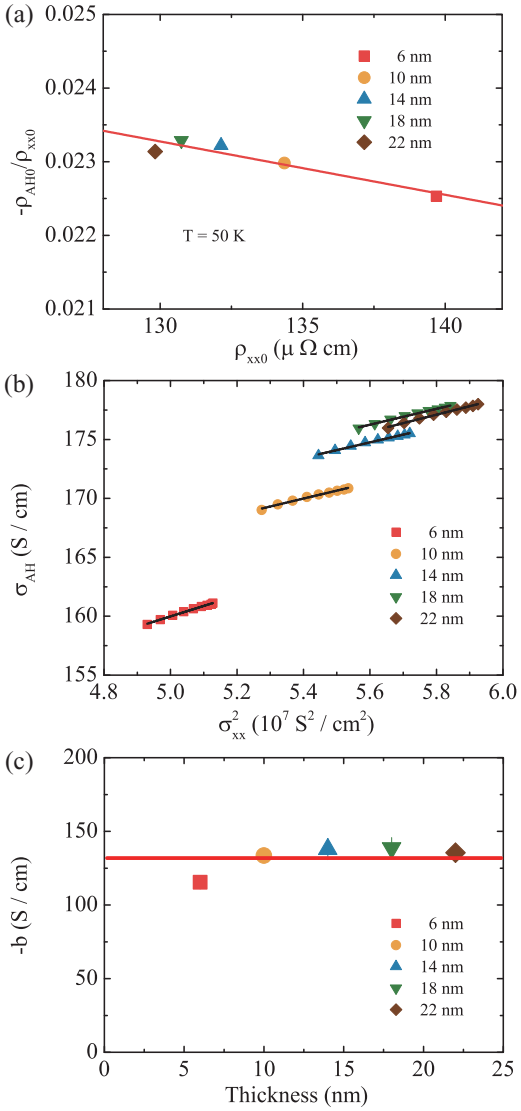

FIG. 3. (Color online) (a) $-\rho_{AH0}/\rho_{xx0}$ versus ρ_{xx0} are given by the dots. ρ_{xx0} are the longitudinal resistivity at 50 K; the red line is the linear fit by $\rho_{AH0}/\rho_{xx0} = \alpha + (\beta + b)\rho_{xx0}$. The intercept is parameter α and the slope is $\beta + b$. (b) σ_{AH} vs σ_{xx}^2 for different thicknesses of CoFeB films. (c) The fitting result for intercept $b(-130 \pm 9$ S/cm) from (b).

of conductivity, the equivalent of Eq. (1) is expressed as

$$\sigma_{AH} = -\left(\alpha\sigma_{xx0}^{-1} + \beta\sigma_{xx0}^{-2}\right)\sigma_{xx}^2 - b. \tag{2}$$

For a CoFeB film with a certain thickness, the residual conductivity σ_{xx0} is fixed, as well as the parameters α and β, thus σ_{AH} is linearly proportional to σ_{xx}^2. In Fig. 3(b) we plot σ_{AH} as a function of σ_{xx}^2. It is seen from the figure that for all the films with different thicknesses the experimental data agree well with the linear fitting, from which the intrinsic AHC b derived from the fittings are presented in Fig. 3(c), and found to be almost constant (-130 ± 9 S/cm). This is consistent with the idea of the intrinsic AHC as a scattering-independent term. The skew scattering and the side jump contribute about -230 and 190 S/cm to the AHC, respectively. Indeed we observed here that the intrinsic contribution is smaller than

the skew scattering term. Presumably this is due to the fact that the absence of the periodic structure in amorphous CoFeB makes the k-space Berry curvature ill defined, and therefore significantly reduces the intrinsic contribution; or the small intrinsic AHE is coming from the real space instead of the k-space Berry curvature, because of the nearest neighbor ordering in CoFeB.

At last it should be mentioned that in literature the empirical $\sigma_{\mathrm{AH}} \propto \sigma_{xx}^{1.6}$ scalings are usually obtained by changing the chemical composition of the compound or alloy under investigation. However, it is well known that the intrinsic contribution b in Eq. (1) is material dependent, or in other words it is composition sensitive too. And it is shown in a recent work that even at the same composition the intrinsic contribution can be strongly modulated by the long range chemical ordering [35]. Therefore, in principle, there is no well-defined scaling at all between ρ_{AH} and ρ_{xx} similar to Eq. (1), if the latter is tuned by the chemical composition. On the other hand, the current approach by the finite size effect of the film resistivity is well defined, once the films are thick enough for the bulklike electronic structure of the materials to be well developed so that the intrinsic AHC is a constant.

To conclude, in contrast to the conventional belief that the AHE in the dirty regime ($\sigma_{xx} < 10^4$ S/cm) can only be described by the phenomenological scaling $\sigma_{\mathrm{AH}} \propto \sigma_{xx}^{1.6}$, we found that for amorphous $Co_{40}Fe_{40}B_{20}$ films which lie in the dirty regime, the AHE can also be quantitatively explained by a combination of the extrinsic and intrinsic mechanisms. It therefore implies that it is possible to understand the AHE under a unified theoretical framework.

This work was supported by MOST (Grant No. 2011CB921802) and NSFC (Grants No. 11374057 and No. 11274371).

[1] K. W. Edmonds, K. Y. Wang, R. P. Campion, A. C. Neumann, C. T. Foxon, B. L. Gallagher, and P. C. Main, Appl. Phys. Lett. **81**, 3010 (2002).
[2] K. Ueno, T. Fukumura, H. Toyosaki, M. Nakano, and M. Kawasaki, Appl. Phys. Lett. **90**, 072103 (2007).
[3] T. Slupinski, H. Munekata, and A. Oiwa, Appl. Phys. Lett. **80**, 1592 (2002).
[4] D. Chiba, M. Yamanouchi, F. Matsukura, and H. Ohno, Science **301**, 943 (2003).
[5] H. Ohno, D. Chiba, F. Matsukura, T. Omiya, E. Abe, T. Dietl, Y. Ohno, and K. Ohtani, Nature (London) **408**, 944 (2000).
[6] J. Smit, Physica **21**, 877 (1955).
[7] L. Berger, Phys. Rev. B **2**, 4559 (1970).
[8] R. Karplus and J. M. Luttinger, Phys. Rev. **95**, 1154 (1954).
[9] T. Jungwirth, Q. Niu, and A. H. MacDonald, Phys. Rev. Lett. **88**, 207208 (2002).
[10] S. Onoda, N. Sugimoto, and N. Nagaosa, Phys. Rev. Lett. **97**, 126602 (2006).
[11] T. Miyasato, N. Abe, T. Fujii, A. Asamitsu, S. Onoda, Y. Onose, N. Nagaosa, and Y. Tokura, Phys. Rev. Lett. **99**, 086602 (2007).
[12] S. Onoda, N. Sugimoto, and N. Nagaosa, Phys. Rev. B **77**, 165103 (2008).
[13] A. Fernández-Pacheco, J. M. De Teresa, J. Orna, L. Morellon, P. A. Algarabel, J. A. Pardo, and M. R. Ibarra, Phys. Rev. B **77**, 100403 (2008).
[14] D. Venkateshvaran, W. Kaiser, A. Boger, M. Althammer, M. S. Ramachandra Rao, S. T. B. Goennenwein, M. Opel, and R. Gross, Phys. Rev. B **78**, 092405 (2008).
[15] S. Iguchi, N. Hanasaki, and Y. Tokura, Phys. Rev. Lett. **99**, 077202 (2007).
[16] N. Nagaosa, J. Sinova, S. Onoda, A. H. MacDonald, and N. P. Ong, Rev. Mod. Phys. **82**, 1539 (2010).
[17] X.-J. Liu, X. Liu, and J. Sinova, Phys. Rev. B **84**, 165304 (2011).
[18] A. Crépieux and P. Bruno, Phys. Rev. B **64**, 014416 (2001).
[19] Y. Tian, L. Ye, and X. Jin, Phys. Rev. Lett. **103**, 087206 (2009).
[20] A. Shitade and N. Nagaosa, J. Phys. Soc. Jpn. **81**, 083704 (2012).
[21] L. Ye, Y. Tian, X. Jin, and D. Xiao, Phys. Rev. B **85**, 220403 (2012).
[22] D. Hou, Y. Li, D. Wei, D. Tian, L. Wu, and X. Jin, J. Phys.: Condens. Matter **24**, 482001 (2012).
[23] L. Wu, Y. Li, J. Xu, D. Hou, and X. Jin, Phys. Rev. B **87**, 155307 (2013).
[24] Y. Li, N. Kanazawa, X. Z. Yu, A. Tsukazaki, M. Kawasaki, M. Ichikawa, X. F. Jin, F. Kagawa, and Y. Tokura, Phys. Rev. Lett. **110**, 117202 (2013).
[25] D. D. Djayaprawira, K. Tsunekawa, M. Nagai, H. Maehara, S. Yamagata, N. Watanabe, S. Yuasa, Y. Suzuki, and K. Ando, Appl. Phys. Lett. **86**, 092502 (2005).
[26] Y. M. Lee, J. Hayakawa, S. Ikeda, F. Matsukura, and H. Ohno, Appl. Phys. Lett. **90**, 212507 (2007).
[27] S. Ikeda, K. Miura, H. Uamamoto, K. Mizunuma, H. D. Gan, M. Endo, S. Kanai, J. Hayakawa, F. Matsukura, and H. Ohno, Nat. Mater. **9**, 721 (2010).
[28] W. Wang, M. Li, S. Hageman, and C. L. Chien, Nat. Mater. **11**, 64 (2011).
[29] B. F. Miao, S. Y. Huang, D. Qu, and C. L. Chien, Phys. Rev. Lett. **111**, 066602 (2013).
[30] E. Saitoh, M. Ueda, H. Miyajima, and G. Tatara, Appl. Phys. Lett. **88**, 182509 (2006).
[31] D. Hou, Z. Qiu, K. Harii, Y. Kajiwara, K. Uchida, Y. Fujikawa, H. Nakayama, T. Yoshino, T. An, K. Ando *et al.*, Appl. Phys. Lett. **101**, 042403 (2012).
[32] A. A. Cottey, Thin Solid Films **1**, 297 (1968).
[33] J. Xu, Y. Li, D. Hou, L. Ye, and X. Jin, Appl. Phys. Lett. **102**, 162401 (2013).
[34] Y. Li, G. Su, D. Hou, L. Ye, Y. Tian, J. Xu, and X. Jin, arXiv:1404.1139.
[35] L. J. Zhu, D. Pan, and J. H. Zhao, Phys. Rev. B **89**, 220406 (2014).